Exploring the Effects of Color Maps on Stitching Close-Range Thermal Images of Solar Panels

***Abstract*—Image mosaicing has been widely used across various fields, but significant challenges persist in thermal imaging, especially for close-range images. These challenges are particularly relevant in solar panel inspections, where precise thermal image stitching is crucial for identifying defects and ensuring optimal performance. This paper investigates the impact of color maps on the stitching quality of close-range thermal images of solar panels. We evaluate eleven color maps and three range selection strategies using a consistent mosaicing dataset. The outputs are compared to RGB-transformed stitched images to quantitatively determine the best color map options. Our findings show that focusing the color map range on the most frequent values significantly improves mosaic quality. Among the color maps tested, Magma and Inferno consistently performed well across all metrics. These results highlight the importance of color map selection in enhancing the accuracy and effectiveness of thermal image mosaicing for solar panel inspection and maintenance.**

I. Introduction

Image stitching is a process in which individual images are combined into one wide-angle mosaic. Much research has already been done in image mosaicing, and methods of quantitatively evaluating these mosaics have been proposed [3]. Thermal image mosaicing is notably more arduous. Temperature magnitudes are visualized through color mappings, and the reconstructed images suffer from fewer visible features due to degradation phenomena [16]. This means that images easily stitched in RGB may result in a lower-quality mosaic or even failure when stitched in their thermal representation.

Solar panels do not demonstrate much feature variation, especially when photographed at close range. Furthermore, sun flares and the surrounding environment frequently cause artifacts to appear in the thermal images, significantly skewing the color map towards the higher temperature values and losing the most relevant features in the process.

In this work, we attempt to increase the stitching quality of close-range thermal solar panel images by optimizing the color map used to represent them. To achieve this, we experimented with the color map and the range of values used in the colorization of the image. Color maps of images that will be stitched together must ideally have the same range. To pick that range, we compared three strategies: full range, averaged range, and focused range. We predicted that focused ranges would prove most effective as they help eliminate unwanted artifacts (e.g., hot spots) and focus on the temperature variations in the solar panel surface, constituting the more significant part of the images in our dataset. The strategies mentioned above were tested on eleven popular thermal color maps, including sequential color maps, cyclic color maps, and a few miscellaneous ones offered by imaging libraries.

One of the biggest hurdles in quantitative evaluation is the lack of ground truth due to the nature of image datasets [7]. Many studies propose methods for substituting ground truth [10]. In this study, we use RGB stitching as a reference for our thermal mosaics, enabling a more accurate comparison between RGB and thermal stitching.

II. Related Work

Image stitching has been widely explored, with new techniques being proposed regularly [2], [3]. To the best of our knowledge, our work is the first study focusing on the application of image stitching for photovoltaic (PV) panels.

To assess the quality of image stitching techniques in different domains, several metrics have been proposed. For example, the Structural Similarity Index, SSIM, was first introduced by Wang et al. [9], then used in many papers to evaluate the performance of image mosaicing algorithms and software [6], [7], [10], [15]. Peak-Signal-to-Noise ratio, or PSNR, is another recurring metric [4], [7], [10], [15], as well as Mutual Information [4], [10] and Entropy [10], [15].

With regard to ground truth, most works evaluating stitching techniques often propose a workaround. Boutellier et al. proposed simulating the imaging process by creating a sequence of mosaic pieces from one reference image, then using that reference as ground truth [6]. Paalanen et al. suggested a similar approach of creating artificial video images via a virtual camera scanning a base image and then using that base image as ground truth [1]. In Sharma et al., rather than create a ground truth, authors opted to bypass the need for it by conducting their evaluation via a comparison between the input images and the output mosaic [7]. Specifically, they compares the overlapping and non-overlapping regions of the two input images against the corresponding areas of the resulting mosaic.

Generally speaking, image mosaics are typically evaluated either via the objective method, the subjective method, or a combination of both. The subjective method requires human resources and is naturally much more expensive and time-consuming. Instead, in this work we evaluate the results of our experimentation objectively using the most commonly used metrics in the literature.

III. Performance Evaluation Method

In this section, we detail the evaluation metrics used to assess the quality of the image mosaic. Our evaluation framework comprises two categories of metrics. The first category

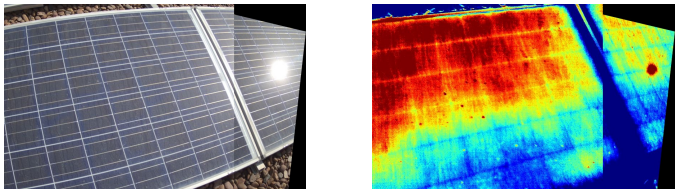

(a) RGB Mosaic (b) Adapted Thermal Mosaic

Fig. 1: Example of thermal ground truth adaption from RGB mosaics

measures the quality of the mosaic based on texture, blurriness, and the richness of information. The second category involves direct comparison with a ground truth image. Given the absence of objective ground truth for each pair of input thermal images, we adopt an innovative approach by computing the homography using the RGB versions of these images. We then apply this homography to stitch the color-mapped thermal representations, creating a pseudo-ground truth for our evaluation. Consequently, we compare the results of our thermal stitching against the corresponding RGB-stitched mosaic for metrics requiring a reference image. This methodology allows us to rigorously evaluate the effectiveness of homography estimation techniques in the thermal domain using a robust and practical framework.

The five quantitative evaluation metrics used in this study are the following.

1) Entropy quantifies the amount of information in an image and does not require a reference to compare against. High entropy indicates a higher level of detail, and low entropy indicates uniformity and lack of information. Entropy is calculated as follows:

$$\text{Entropy} = -\sum_{i=1}^{n} p(x_i) \log_2 p(x_i) \tag{1}$$

Where $p(x_i)$ is the probability of the ith gray-scaled intensity value.

2) Clarity quantifies the sharpness and definition of an image, typically using some form of edge detection. The higher the clarity of the mosaic, the less blurry it is. Like entropy, clarity does not require a reference image.

$$\begin{aligned} G &= \sqrt{\frac{\partial I}{\partial x}^2 + \frac{\partial I}{\partial y}^2} \\ \text{Clarity} &= \sum_{i=1}^{M}\sum_{j=1}^{N} G_{i,j} \end{aligned} \tag{2}$$

3) Peak-Signal-to-Noise-Ratio (PSNR), is one of the most popular evaluation metrics for image mosaicing. It compares a reconstructed image with a reference to measure its fidelity. The higher the PSNR value, the closer the mosaic is to the reference.

$$\begin{aligned} \text{MSE} &= \frac{1}{MN}\sum_{i=0}^{M-1}\sum_{j=0}^{N-1}[I(i,j) - K(i,j)]^2 \\ \text{PSNR} &= 20 \cdot \log_{10}\left(\frac{255}{\sqrt{\text{MSE}}}\right) \end{aligned} \tag{3}$$

4) The Structural Similarity Index (SSIM) is another popular image mosaicing metric that focuses on luminance and contrast, taking into account Weber's law regarding the human visual system [9]. The higher the value of SSIM, the more structurally similar the mosaic is to the reference, with a value of 1 indicating identical images.

$$\begin{aligned} l(x,y) &= \frac{2\mu_x\mu_y + C_1}{\mu_x^2 + \mu_y^2 + C_1} \\ c(x,y) &= \frac{2\sigma_x\sigma_y + C_2}{\sigma_x^2 + \sigma_y^2 + C_2} \\ s(x,y) &= \frac{\sigma_{xy} + C_3}{\sigma_x\sigma_y + C_3} \end{aligned} \tag{4}$$

$$\text{SSIM}(x,y) = [l(x,y)]^\alpha \cdot [c(x,y)]^\beta \cdot [s(x,y)]^\gamma$$

5) Mutual Information (MI) is a measurement of similarity between the mosaic and a reference, with a higher value indicating a more significant amount of shared information. MI is calculated via the marginal and joint probability distributions of the two images.

$$MI(X;Y) = \sum_{y\in Y}\sum_{x\in X} p(x,y)\log\left(\frac{p(x,y)}{p(x)p(y)}\right) \tag{5}$$

Most of these metrics gained popularity with RGB image mosaicing. Thermal mosaicing has inherently fewer defined features, meaning that these metrics will not perform as well as expected. Furthermore, a challenge we encountered while dealing with close-range solar panel thermal images is that the metrics requiring a reference comparison, MI especially, could favor simpler, smoother images that avoid much of the discrepancies more feature-heavy images introduce. To that end, while we do compute all the measurements mentioned above, we do expect some disparity when it comes to full-range color maps, which can sometimes lose most if not all, discernible features.

IV. Dataset and Methodology

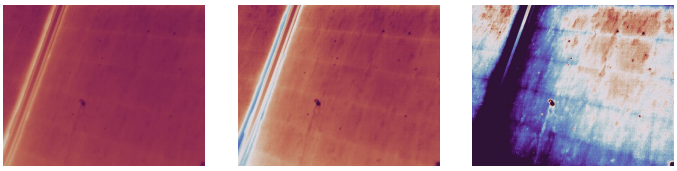

(a) Full Range (b) Averaged Range (c) Focused Range

Fig. 2: Examples of the three ranges applied to the same image.

The dataset used in this paper consists of fourteen different sequences of radiometric images, all together making up 56 possible mosaic pairs. Radiometric images contain thermal and visible data in a single file, which allows us to construct the reference mosaics used for ground truth as previously described. The dataset contains images taken from a 10-30 centimeter distance from the solar panels by moving the camera horizontally across and from one stationary position with the camera panning around that center. All 56 image pairs were inputted into a traditional SIFT-based stitching pipeline.

Three color map ranges and eleven color maps were tested using the dataset. The three range selection strategies were as follows:

1) Full range, where we determine the lowest and highest thermal value in the stitched sequence. That would then be the minimum and maximum values in the color map. This method ensured that no thermal information was outside the map range. Still, the RGB limits of a color map dictated that the more values the range includes, the less visually differentiated they would be.
2) Averaged range, where we determined the lowest thermal values in each image of a sequence, then set the color map's minimum to the average of said values, and likewise for the maximum. This attempted to constrict the full range into a more visually differentiated one. However, the presence of recurring sun flares in multiple images may reduce the effectiveness of this approach.
3) Focused range, where we first limit the thermal values of each image to the 70 most frequently occurring ones, and then we get a full range on that subset of values. This comes at the expense of much of the thermal variation in each image. However, with solar panels, more often than not, the majority of close-range photos consist of a visually uniform panel. Focusing on that allows us to distinguish the slight thermal variations better, revealing features where none existed. One frequent example of this is the thermal differentiation of the busbars, which becomes evident only when the focused range is used. This is demonstrated in Figure 2.

Our evaluation uses color maps: Hot, Inferno, Magma, Plasma, Viridis, Cividis, HSV, Twilight Shifted, Twilight, CMRmap, and Jet. Hot, Inferno, Magma, Plasma, Viridis, and Cividis are all sequential maps, where the lightness values monotonically increase. Twilight and Twilight Shifted are cyclic maps that monotonically change lightness until the halfway point and then symmetrically change back. HSV is included as a cyclic color map, though it is not entirely symmetric in lightness. CMRmap is a map specifically designed to convert well to grayscale. Jet is a popular map famous for rapid color and brightness changes emphasizing less visible details.

V. Experimental Results

Figure 3 displays the average metric values for each range option, the standard deviation of that mean, and the metric value of the best-performing color map in that range category.

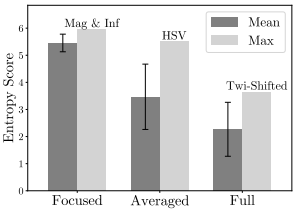

(a) Entropy Range Evaluation

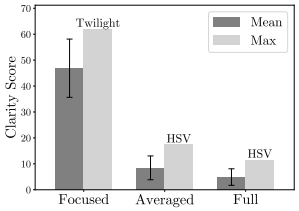

(b) Clarity Range Evaluation

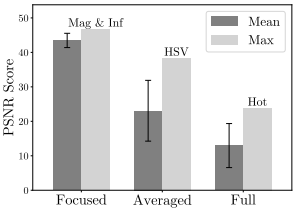

(c) PSNR Range Evaluation

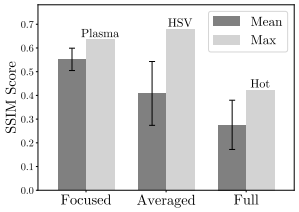

(d) SSIM Range Evaluation

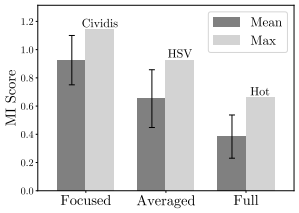

(e) MI Range Evaluation

Fig. 3: Evaluation results across all color maps.

Overall, the focused range mostly outperforms the averaged and full ranges, with a few exceptions, as predicted. In particular, the focused range combined with the Hot color map yields a marginally lower MI score than the entire range, and the Jet color map yields lower than the averaged range. Another surprising result is with the HSV color map, where entropy, MI, and SSIM are all lower for the focused range than for the averaged range.

Interestingly, the color maps Magma and Inferno yielded identical results across all five metrics, likely due to near-identical lightness levels throughout. The two color maps were also the only ones to rank consistently among the top five values for each metric. Also interesting to note is that HSV dominated the ranks for averaged ranges with exceptional scores. We can attribute this to using only a small sub-range of the HSV colors due to the existence of hot spots. In a color map as rich and contrasted as HSV, it was likely an improvement to limit the color range.

The stitching pipeline would often fail to stitch due to a lack of detected features. This happened more frequently when testing the color maps with full or averaged ranges. The percentages of failed stitching corresponding to each color map and range are displayed in Table I.

VI. Conclusions and Future Work

This study has shown that focusing on a color map range limited to the most frequently occurring thermal values in

TABLE I: Failure Percentages for Different Color Maps

Color Map	Failure %	Color Map	Failure %
Hot focused	0.0%	Magma focused	1.8%
Hot averaged	57.1%	Magma averaged	51.8%
Hot full	58.9%	Magma full	78.6%
Inferno focused	1.8%	Plasma focused	5.4%
Inferno averaged	51.8%	Plasma averaged	67.9%
Inferno full	42.9%	Plasma full	80.4%
Jet focused	0.0%	Viridis focused	14.3%
Jet averaged	35.7%	Viridis averaged	78.6%
Jet full	67.9%	Viridis full	91.1%
Cividis focused	5.4%	Twilight focused	0.0%
Cividis averaged	75.0%	Twilight averaged	33.9%
Cividis full	85.7%	Twilight full	66.1%
HSV focused	0.0%	CMRmap focused	3.6%
HSV averaged	16.1%	CMRmap averaged	57.1%
HSV full	53.6%	CMRmap full	78.6%
Twi-Shifted focused	0.0%		
Twi-Shifted averaged	32.1%		
Twi-Shifted full	58.9%		

close-range solar panel images significantly improves the resulting mosaics. Concentrating on this small range enhances the visibility of slight thermal variations in the panels, leading to better-defined features for stitching. Among the tested color maps, perceptually uniform sequential color maps such as Magma, Inferno, Plasma, Viridis, and Cividis often yielded the best scores, likely due to their uniformly increasing lightness levels.

The results indicate that the focused range method outperforms the averaged and full-range methods across metrics such as entropy, clarity, PSNR, SSIM, and MI. These findings highlight the importance of color map selection and range focusing in thermal image mosaicing, particularly for applications where fine thermal details are crucial. However, we encountered limitations such as challenges in stitching images with fewer visible features and occasional stitching failures, underscoring the need for further research. The disparities observed in metrics like MI and SSIM for different color maps suggest that some metrics may favor certain visual characteristics over others, particularly in thermal imaging.

While this paper demonstrates the effectiveness of focused color map ranges and specific color maps for improving the stitching quality of close-range thermal solar panel images, several avenues for future research remain. Future studies should test this approach in other thermal imaging contexts, both close and far-range, with varying image characteristics.

Further research should improve the stitching pipeline's robustness by experimenting with different feature detection and stitching algorithms beyond SIFT. Additionally, investigating the impact of various color maps, including the development of custom color maps, could further enhance the quality of close-range thermal image mosaics.

Finally, the performance metrics used in this study were originally designed for RGB images and may not fully capture the nuances of thermal imaging. Future research could focus on developing or adapting metrics specifically for thermal images to provide more accurate and meaningful assessments of stitching quality.

In summary, this study developed a framework to improve the creation of close-range thermal image mosaics by optimizing color map ranges and selecting appropriate color maps. These findings have the potential to enhance a wide range of thermal imaging applications in the future, leading to more accurate and detailed thermal mosaics in various fields.

REFERENCES

[1] P. Paalanen, J.-K. Kämäräinen, and H. Kälviäinen, "Image Based Quantitative Mosaic Evaluation with Artificial Video," in *Image Analysis*, A.-B. Salberg, J. Y. Hardeberg, and R. Jenssen, Eds. Berlin, Heidelberg: Springer Berlin Heidelberg, 2009, pp. 470-479. doi: 10.1007/978-3-642-02230-2

[2] A. Pandey and U. C. Pati, "Image mosaicing: A deeper insight," *Image and Vision Computing*, vol. 89, pp. 236-257, 2019. doi: 10.1016/j.imavis.2019.07.002

[3] D. Ghosh and N. Kaabouch, "A survey on image mosaicing techniques," *Journal of Visual Communication and Image Representation*, vol. 34, pp. 1-11, 2016. doi: 10.1016/j.jvcir.2015.10.014

[4] D. Ghosh, S. Park, N. Kaabouch, and W. Semke, "Quantitative evaluation of image mosaicing in multiple scene categories," in *2012 IEEE International Conference on Electro/Information Technology*, 2012, pp. 1-6. doi: 10.1109/EIT.2012.6220726

[5] P. Azzari, L. Di Stefano, and S. Mattoccia, "An Evaluation Methodology for Image Mosaicing Algorithms," in *Advanced Concepts for Intelligent Vision Systems*, J. Blanc-Talon et al., Eds. Berlin, Heidelberg: Springer Berlin Heidelberg, 2008, pp. 89-100. doi: 10.1007/978-3-540-88458-3

[6] J. Boutellier, O. Silvén, M. Tico, and L. Korhonen, "Objective Evaluation of Image Mosaics," in *Computer Vision and Computer Graphics. Theory and Applications*, J. Braz et al., Eds. Berlin, Heidelberg: Springer Berlin Heidelberg, 2008, pp. 107-117. doi: 10.1007/978-3-540-89682-1

[7] S. K. Sharma, K. Jain, and M. Suresh, "Quantitative Evaluation of Panorama Softwares," in *ICCCE 2018*, A. Kumar and S. Mozar, Eds. Singapore: Springer Singapore, 2019, pp. 543-561. doi: 10.1007/978-981-13-0212-1

[8] Y. Yang and X. Lee, "Four-band Thermal Mosaicking: A New Method to Process Infrared Thermal Imagery of Urban Landscapes from UAV Flights," *Remote Sensing*, vol. 11, no. 11, article 1365, 2019. doi: 10.3390/rs11111365

[9] Z. Wang, A. C. Bovik, H. R. Sheikh, and E. P. Simoncelli, "Image quality assessment: from error visibility to structural similarity," *IEEE Transactions on Image Processing*, vol. 13, no. 4, pp. 600-612, 2004. doi: 10.1109/TIP.2003.819861

[10] W. Zhang, J. Li, and Z. Zhang, "Performance evaluation approach for image mosaicing algorithm," in *2013 25th Chinese Control and Decision Conference (CCDC)*, 2013, pp. 3786-3791. doi: 10.1109/CCDC.2013.6561608

[11] J. Cui, M. Liu, Z. Zhang, S. Yang, and J. Ning, "Robust UAV Thermal Infrared Remote Sensing Images Stitching Via Overlap-Prior-Based Global Similarity Prior Model," *IEEE Journal of Selected Topics in Applied Earth Observations and Remote Sensing*, vol. 14, pp. 270-282, 2021. doi: 10.1109/JSTARS.2020.3032011

[12] X. Jin, C. Wang, G. Han, Y. Wang, and J. Jia, "A Novel Stitching Method for High-Precision Low-Overlap Thermal Infrared Array Sweeping Images," *IEEE Transactions on Geoscience and Remote Sensing*, vol. 62, pp. 1-17, 2024. doi: 10.1109/TGRS.2023.3337244

[13] S. Yahyanejad and B. Rinner, "A fast and mobile system for registration of low-altitude visual and thermal aerial images using multiple small-scale UAVs," *ISPRS Journal of Photogrammetry and Remote Sensing*, vol. 104, pp. 189-202, 2015. doi: 10.1016/j.isprsjprs.2014.07.015

[14] J. Yu, Y. He, F. Zhang, G. Sun, Y. Hou, H. Liu, J. Li, R. Yang, and H. Wang, "An Infrared Image Stitching Method for Wind Turbine Blade Using UAV Flight Data and U-Net," *IEEE Sensors Journal*, vol. 23, no. 8, pp. 8727-8736, 2023. doi: 10.1109/JSEN.2023.3257824

[15] L.-h. Zou, J. Chen, and J. Zhang, "Assessment approach for image mosaicing algorithms," *Optical Engineering*, vol. 50, no. 11, article 110501, 2011. doi: 10.1117/1.3646746

[16] C. Yin, X. Huang, X. Tan, and J. Liu, "Stitching Technique for Reconstructed Thermal Images," in *Infrared Thermographic NDT-based Damage Detection and Analysis Method for Spacecraft*, Singapore: Springer Nature Singapore, 2024, pp. 93-129. doi: 10.1007/978-981-99-8216-5_4